

Synthesis, Characterization and Evaluation of Anticancer Activity of New Pyrazole-5-carboxamide Derivatives

J. PRATHYUSHA*^{ORCID} and C. ASHA DEEPTI^{ORCID}

Department of Pharmaceutical Chemistry, Gitam School of Pharmacy, GITAM Deemed to be University, Visakhapatnam-530045, India

*Corresponding author: E-mail: prathyusha.rj@gmail.com

Received: 31 May 2023;

Accepted: 21 July 2023;

Published online: 31 July 2023;

AJC-21338

In recent years, pyrazole derivatives have emerged as a potentially game-changing new family of cancer chemotherapeutic drugs. Thus, present work used six distinct cancer cell lines to test the new pyrazole-5-carboxamide derivatives for the anticancer activity. Present study includes synthesis, characterization and the ligand-based molecular docking of the compounds. The process begins with ethyl 2,4-dioxopentanoate and methylhydrazine, which was cyclized to form ethyl 1,3-dimethyl-1H-pyrazole-5-carboxylate (**2**), which is then transformed to 1,3-dimethyl-1H-pyrazole-5-carbonyl chloride (**3**) through PCl_5/I_2 . All the pyrazole-4-carboxamides (**4a-n**) were obtained by the acidic condensation of intermediate **3** with various substituted aryl amines (**a-n**). The antitumor activity against six cancer cell lines and one regular human cell line was measured using the MTT test. Two target proteins, human *c*-Met kinase and JAK1, were used in docking studies of the proposed compounds. When compared against the standard drug doxorubicin, most of the synthesized compounds (**4a-n**) showed the promising cytotoxicity profiles.

Keywords: Pyrazole-5-carboxamide, Anticancer activity, Molecular docking, Doxorubicin.

INTRODUCTION

Amounting to the number of deaths to 10 million in the year 2020 globally, cancer has become the second leading cause of global mortality. Among the numerous types of cancer, breast, lung, colon, prostate and skin are the leading incidence of the number of new cases, while the lung and colon cancers are leading the number of deaths. Cancer continues to be a major disorder threatening human health despite significant advances in cancer treatment strategies [1].

Among the main strategies used to reduce cancer, chemotherapy is an essential and feasible approach due to its basicness compared to other, more intricate methods such as surgery and radiotherapy [2]. Although many anticancer chemotherapy drugs are effective in treating a wide range of conditions of cancer, the short-term and long-term consequences sequelae of anticancer drugs has become a significant concern for both patients and physicians [3]. In some cases, strategies to combat the anticancer drug's side effects are practical but don't address the longer-term sequelae. It is, therefore, imperative to develop target-specific, tolerable and compelling new anticancer agents to address this challenge [4].

The concept of a chemical scaffold as a basic structure directly related to the pharmacological profile of a drug is an essential tool for researchers in medicinal chemistry and it becomes a vital approach in the anticancer drug design process [5,6]. Heterocyclic scaffolds have been considered as preferred structures in the development of numerous approved anticancer medicines due to their structural similarities with one another [7]. Among the heterocyclics, the compounds with nitrogen atoms in their structures represent the largest class ofazole family. Pyrazole is a five membered aromatic hetero-cyclic compound containing two adjacent nitrogens and two endocyclic double bonds particularly helpful for the organic synthesis. They are specifically referred to as antiviral, antioxidant, anti-tuberculosis, antiphlogistic, anti-depressant, anti-inflammatory, analgesic, anticancer, antifungal, antibacterial, antidiabetic, acaricidal, insecticidal, antiparasitic, antifungal agents and protein glycation inhibitors [8]. Several pyrazole analogues present in many natural and synthetic molecules act like protein kinase, HIV-1 reverse transcriptase and COX-2 inhibitors. Due to their intriguing pharmacological properties, pyrazole derivatives as biomolecules have recently received

increased attention. Numerous well-known medications from various categories with a range of therapeutic effects contain this heterocycle [9].

After thiazole and pyrimidine, pyrazole scaffold is the most investigated moiety in anticancer research [10-14]. Because of their potent inhibition of BRAF (V600E), GFR, telomerase, pyrazole derivatives ROS receptor tyrosine kinase and Aurora-A kinase are widely used as anticancer medicines [15]. Recently, two pyrazole-bearing anticancer drugs, the FDA has given its blessing to both ruxolitinib and crizotinib. Myelofibrosis with intermediate or high risk, polycythemia vera and graft-versus-host disease with resistant forms are all treated with ruxolitinib, a small molecule Janus kinase inhibitor [16]. Selective tyrosine kinase receptor inhibitor crizotinib is used to treat some forms of advanced non-small cell lung cancer [17].

Carboxamide substituted pyrazoles are considered as important scaffolds as they have the property of reversibly binding to proteins and also their structure mimic with peptides structure [18]. Pyrazole-carboxamide derivatives can be easily synthesized with high yields and have bioactivity in the sub micromolar range which drag the attention of the many researchers [19].

EXPERIMENTAL

Chemicals employed for the synthesis were procured from Sigma-Aldrich, USA. Reaction was checked by using Merck-precoated aluminium TLC plates of silica gel 60 F₂₅₄ and the spots were visualized with iodine vapours in the UV chamber. Purification and isolation of the synthesized compounds were done by using column chromatography. The Remi electronic melting point apparatus was used to determine the melting points and are uncorrected. ¹H NMR was recorded on BRUKER DRX-500 MHz. Chemical shift values (δ) in ppm and tetramethyl silane (TMS) was used as a reference internal standard. The MASS spectra were recorded on BRUKER ESI-IT MS.

Synthesis of ethyl 1,3-dimethyl-1H-pyrazole-5-carboxylate (2): Ethyl 2,4-dioxopentanoate (46.5 g) was dissolved in anhydrous ethanol (300 mL) at 5 °C with stirring. The solution was then agitated at 0 °C for 2 h while 0.38 mol of methylhydrazine was added gently in water. Under vacuum, the solvent was evaporated and then ethyl acetate was used to extract the aqueous phase. After thorough washing with water, drying over Na₂SO₄, filter and concentrated under low pressure, product 2 was obtained as yellow solid (yield: 39.3 g, 92% and 90% purity).

Synthesis of 1,3-dimethyl-1H-pyrazole-5-carbonyl chloride (3): For 12 h at 1000 °C with vigorous stirring, 1,3-

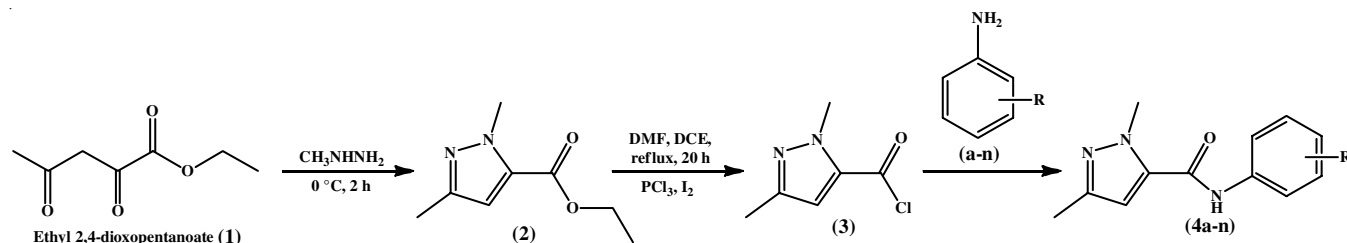
dimethyl-1H-pyrazole-5-carboxylate (2) (1.3 mmol), PCl₃ (1.3 mmol), iodine (0.13) mmol and DMF (2.6 mmol) were mixed. Compound 3 was obtained by evaporating the RBF's contents, working them up with water, extracting them with hexane and purifying the resulting mixture through column chromatography.

Synthesis of 1H-pyrazole-5-carboxamide derivatives (4a-n): In the acidic environment, 20 mL ethanolic solution of compound 3 (1 mmol, 1 equiv.) was refluxed with substituted aromatic amines (1 mmol, 1 equiv.). After the reaction was completed, the crude mass was washed by using NaHCO₃ solution and extracted with three equal volumes of ethyl acetate (Scheme-I). Brine solution was used to treat the organic layer and then evaporated under vacuum and column chromatography was used to purify 1H-pyrazole-5-carboxamide derivatives (4a-n) by using 10% ethyl acetate-hexane as mobile phase [20].

1,3-Dimethyl-N-phenyl-1H-pyrazole-5-carboxamide (4a): Colour: pale yellow solid: yield: 74%; m.p.: 162-163 °C. FT-IR (KBr, ν_{\max} , cm⁻¹) 3352 (NH *str.*), 3010 (Ar-CH *str.*), 2940 (aliph. CH *str.*), 1690 (C=O), 1638 (C=N), 1495 (C=C), 1310 (C-N); ¹H NMR (500 MHz, CDCl₃) δ ppm: 2.34 (s, 3H, CH₃), 3.75 (s, 3H, N-CH₃), 6.40 (s, 1H, CH=C), 7.07 (tt, *J* = 7.8, 1.2 Hz, 1H, Ar-H), 7.27 (dddd, *J* = 8.2, 7.8, 1.4, 0.5 Hz, 2H, Ar-H), 7.49 (dddd, *J* = 8.2, 1.5, 1.2, 0.5 Hz, 2H, Ar-H). ¹³C NMR (300 MHz, CDCl₃) δ ppm: 13.9 (CH₃), 37.7 (N-CH₃), 108.1 (CH=C), 119.9 (2C, Ar-C), 127.8 (Ar-C), 128.2 (2C, Ar-C), 133.7 (C-C=O), 137.4 (Ar-C-NH), 149.9 (N=C-CH), 159.9 (C=O-NH). ESI-MS: *m/z* Anal. calcd. for C₁₂H₁₃N₃O ([M + H]⁺): 215.26, found 216.15.

N-(3-Hydroxyphenyl)-1,3-dimethyl-1H-pyrazole-5-carboxamide (4b): Colour: pale yellow solid: yield: 57%; m.p.: 157-158 °C. FT-IR (KBr, ν_{\max} , cm⁻¹): 3352 (NH *str.*), 3010 (Ar-CH *str.*), 2940 (aliph. CH *str.*), 1688 (C=O), 1640 (C=N), 1495 (C=C), 1310 (C-N); ¹H NMR (500 MHz CDCl₃) δ ppm: 2.34 (s, 3H, CH₃), 3.75 (s, 3H, N-CH₃), 6.40 (s, 1H, CH=C), 6.74 (ddd, *J* = 8.2, 2.2, 1.6 Hz, 1H, Ar-H), 7.23 (td, *J* = 8.2, 0.5 Hz, 1H, Ar-H), 7.32-7.53 (7.38 (ddd, *J* = 2.2, 1.4, 0.5 Hz, Ar-H), 7.47 (ddd, *J* = 8.2, 1.6, 1.4 Hz, Ar-H), 2H). ¹³C NMR (300 MHz, CDCl₃) δ ppm: 13.9 (CH₃), 37.7 (N-CH₃), 105.0 (Ar-C), 108.1 (CH=C), 114.5 (Ar-C), 119.9 (Ar-C), 129.7 (Ar-C), 133.7 (C-C=O), 139.3 (Ar-C-NH), 149.9 (N=C-CH), 157.4 (Ar-C-OH), 159.9 (C=O-NH). ESI-MS: *m/z* Anal. calcd. for C₁₂H₁₃N₃O₂ ([M + H]⁺): 231.25; found: 232.20.

N-(4-Hydroxyphenyl)-1,3-dimethyl-1H-pyrazole-5-carboxamide (4c): Colour: pale yellow solid: yield: 57%; m.p.: 179-180 °C, FT-IR (KBr, ν_{\max} , cm⁻¹): 3352 (NH *str.*), 3010 (Ar-CH *str.*), 2940 (aliph. CH *str.*), 1690 (C=O), 1638 (C=N), 1495 (C=C), 1312 (C-N); ¹H NMR: (500 MHz, CDCl₃) δ ppm: 2.34 (s, 3H, CH₃), 3.75 (s, 3H, N-CH₃), 6.40 (s, 1H, CH=C),



Scheme-I: Synthesis of pyrazole-5-carboxamide derivatives

6.67 (ddd, $J = 8.8, 2.6, 0.6$ Hz, 2H, Ar-H), 7.28 (ddd, $J = 8.8, 1.8, 0.6$ Hz, 2H, Ar-H). ^{13}C NMR (300 MHz, CDCl_3) δ ppm: 13.9 (CH_3), 37.7 (N- CH_3), 108.1 ($\text{CH}=\text{C}$), 115.2 (2C, Ar-C), 120.5 (2C, Ar-C), 133.7 (C-C=O), 137.4 (Ar-C-NH), 149.9 (N=C-CH), 157.4 (Ar-C-OH), 159.9 (C=O-NH). ESI-MS: m/z Anal. calcd. for $\text{C}_{12}\text{H}_{13}\text{N}_3\text{O}_2$ ($[\text{M} + \text{H}]^+$): 231.25; found: 232.20.

***N*-(2-Hydroxyphenyl)-1,3-dimethyl-1*H*-pyrazole-5-carboxamide (4d)**: Colour: pale yellow solid; yield: 59%; m.p.: 147-148 °C, FT-IR (KBr, ν_{max} , cm^{-1}): 3352 (NH *str.*), 3010 (Ar-CH *str.*), 2940 (aliph. CH *str.*), 1690 (C=O), 1638 (C=N), 1495 (C=C), 1310 (C-N); ^1H NMR (500 MHz, CDCl_3) δ ppm: 2.34 (s, 3H, CH_3), 3.75 (s, 3H, N- CH_3), 6.40 (s, 1H, $\text{CH}=\text{C}$), 6.68 (ddd, $J = 8.5, 1.3, 0.5$ Hz, 1H, Ar-H), 6.97-7.21 (7.04 (ddd, $J = 8.5, 7.5, 1.2$ Hz, Ar-H), 7.13 (ddd, $J = 8.3, 7.5, 1.3$ Hz, Ar-H, 2H), 7.37 (ddd, $J = 8.3, 1.2, 0.5$ Hz, 1H, Ar-H)). ^{13}C NMR (300 MHz, CDCl_3) δ ppm: 13.9 (CH_3), 37.7 (N- CH_3), 108.1 ($\text{CH}=\text{C}$), 115.1 (1C, Ar-C), 117.4 (1C, Ar-C), 124.5 (Ar-C-NH), 128.2 (Ar-C), 129.4 (Ar-C), 133.7 (C-C=O), 147.8 (Ar-C-OH), 149.9 (N=C-CH), 159.9 (C=O-NH). ESI-MS: m/z Anal. calcd. for $\text{C}_{12}\text{H}_{13}\text{N}_3\text{O}_2$ ($[\text{M} + \text{H}]^+$): 231.25; found: 232.20.

1,3-Dimethyl-*N*-(3-nitrophenyl)-1*H*-pyrazole-5-carboxamide (4e): Colour: pale yellow solid; yield: 71%; m.p.: 163-164 °C, FT-IR (KBr, ν_{max} , cm^{-1}): 3352 (NH *str.*), 3010 (Ar-CH *str.*), 2940 (aliph. CH *str.*), 1690 (C=O), 1640 (C=N), 1495 (C=C), 1310 (C-N). ^1H NMR (500 MHz, CDCl_3) δ ppm: 2.34 (s, 3H, CH_3), 3.75 (s, 3H, N- CH_3), 6.40 (s, 1H, $\text{CH}=\text{C}$), 7.36-7.52 (dt, $J = 8.2, 1.5$ Hz, Ar-H), 7.45 (ddd, $J = 8.4, 8.2, 0.5$ Hz, Ar-H), 7.45 (ddd, $J = 8.4, 1.7, 1.6$ Hz, Ar-H, 3H), 7.87 (ddd, $J = 1.7, 1.5, 0.5$ Hz, 1H, Ar-H). ^{13}C NMR (300 MHz, CDCl_3) δ ppm: 13.9 (CH_3), 37.7 (N- CH_3), 108.1 ($\text{CH}=\text{C}$), 112.0 (Ar-C), 119.9 (Ar-C), 123.3 (Ar-C), 129.6 (Ar-C), 133.7 (C-C=O), 137.5 (Ar-C-NH), 143.9 (Ar-C- NO_2), 149.9 (N=C-CH), 159.9 (C=O-NH). ESI-MS: m/z Anal. calcd. for $\text{C}_{12}\text{H}_{12}\text{N}_4\text{O}_3$ ($[\text{M} + \text{H}]^+$): 260.25; found: 261.15.

1,3-Dimethyl-*N*-(4-nitrophenyl)-1*H*-pyrazole-5-carboxamide (4f): Colour: pale yellow solid; yield: 73%; m.p.: 174-175 °C, FT-IR (KBr, ν_{max} , cm^{-1}): 3352 (NH *str.*), 3010 (Ar-CH *str.*), 2940 (aliph. CH *str.*), 1690 (C=O), 1638 (C=N), 1480 (C=C), 1310 (C-N); ^1H NMR (500 MHz, CDCl_3) δ ppm: 2.34 (s, 3H, CH_3), 3.75 (s, 3H, N- CH_3), 6.42 (s, 1H, $\text{CH}=\text{C}$), 7.35 (ddd, $J = 8.7, 2.2, 0.4$ Hz, 2H, Ar-H), 8.13 (ddd, $J = 8.7, 1.8, 0.4$ Hz, 2H, Ar-H). ^{13}C NMR (300 MHz, CDCl_3) δ ppm: 13.9 (CH_3), 37.7 (N- CH_3), 108.1 ($\text{CH}=\text{C}$), 116.6 (2C, Ar-C), 125.0 (2C, Ar-C), 133.7 (C-C=O), 137.4 (Ar-C-NH), 147.3 (Ar-C- NO_2), 149.9 (N=C-CH), 159.9 (C=O-NH). ESI-MS: m/z Anal. calcd. for $\text{C}_{12}\text{H}_{12}\text{N}_4\text{O}_3$ ($[\text{M} + \text{H}]^+$): 260.25; found: 261.20.

***N*-(3-Fluorophenyl)-1,3-dimethyl-1*H*-pyrazole-5-carboxamide (4g)**: Colour: pale yellow solid; yield: 70%; m.p.: 132-133 °C, FTIR (KBr, ν_{max} , cm^{-1}): 3352 (NH *str.*), 3010 (Ar-CH *str.*), 2940 (aliph. CH *str.*), 1690 (C=O), 1638 (C=N), 1495 (C=C), 1310 (C-N); ^1H NMR (500 MHz, CDCl_3) δ ppm: 2.34 (s, 3H, CH_3), 3.75 (s, 3H, N- CH_3), 6.40 (s, 1H, $\text{CH}=\text{C}$), 7.01 (ddd, $J = 8.4, 1.7, 1.4$ Hz, 1H, Ar-H), 7.34 (ddd, $J = 8.4, 8.2, 0.5$ Hz, 1H, Ar-H), 7.54 (ddd, $J = 8.2, 1.7, 1.4$ Hz, 1H, Ar-H), 7.72 (td, $J = 1.7, 0.5$ Hz, 1H, Ar-H). ^{13}C NMR (300 MHz, CDCl_3) δ ppm: 13.9 (CH_3), 37.7 (N- CH_3), 108.1 ($\text{CH}=\text{C}$), 110.8 (Ar-C), 115.0 (Ar-C), 119.9 (Ar-C), 129.9 (Ar-C), 133.7 (C-C=O), 139.6

(Ar-C-NH), 149.9 (N=C-CH), 159.9 (C=O-NH), 160.6 (Ar-C-F). ESI-MS: m/z Anal. calcd. for $\text{C}_{12}\text{H}_{12}\text{FN}_3\text{O}$ ($[\text{M} + \text{H}]^+$): 233.25; found: 234.20.

***N*-(4-Fluorophenyl)-1,3-dimethyl-1*H*-pyrazole-5-carboxamide (4h)**: Colour: pale yellow solid; yield: 70%; m.p.: 151-152 °C, FTIR (KBr, ν_{max} , cm^{-1}): 3352 (NH *str.*), 3010 (Ar-CH *str.*), 2940 (aliph. CH *str.*), 1690 (C=O), 1638 (C=N), 1495 (C=C), 1312 (C-N); ^1H NMR (500 MHz, CDCl_3) δ ppm: 2.34 (s, 3H, CH_3), 3.75 (s, 3H, N- CH_3), 6.40 (s, 1H, $\text{CH}=\text{C}$), 7.02 (ddd, $J = 8.6, 1.5, 0.6$ Hz, 2H, Ar-H), 7.75 (ddd, $J = 8.6, 1.8, 0.6$ Hz, 2H, Ar-H). ^{13}C NMR (300 MHz, CDCl_3) δ ppm: 13.9 (CH_3), 37.7 (N- CH_3), 108.1 ($\text{CH}=\text{C}$), 115.6 (2C, Ar-C), 118.2 (2C, Ar-C), 133.7 (C-C=O), 137.4 (Ar-C-NH), 149.9 (N=C-CH), 159.9 (C=O-NH), 162.5 (Ar-C-F). ESI-MS: m/z Anal. calcd. for $\text{C}_{12}\text{H}_{12}\text{FN}_3\text{O}$ ($[\text{M} + \text{H}]^+$): 233.25; found: 234.20.

***N*-(3-Chlorophenyl)-1,3-dimethyl-1*H*-pyrazole-5-carboxamide (4i)**: Colour: pale yellow solid; yield: 67%; m.p.: 155-156 °C, FTIR (KBr, ν_{max} , cm^{-1}): 3352 (NH *str.*), 3010 (Ar-CH *str.*), 2940 (aliph. CH *str.*), 1690 (C=O), 1638 (C=N), 1495 (C=C), 1310 (C-N); ^1H NMR (500 MHz, CDCl_3) δ ppm: 2.34 (s, 3H, CH_3), 3.75 (s, 3H, N- CH_3), 6.40 (s, 1H, $\text{CH}=\text{C}$), 7.15 (dt, $J = 8.1, 1.7$ Hz, Ar-H), 7.35 (td, $J = 8.1, 0.5$ Hz, 1H, Ar-H), 7.59 (dt, $J = 8.2, 1.7$ Hz, 1H, Ar-H), 7.78 (td, $J = 1.7, 0.5$ Hz, 1H, Ar-H). ^{13}C NMR (300 MHz, CDCl_3) δ ppm: 13.9 (CH_3), 37.7 (N- CH_3), 108.1 ($\text{CH}=\text{C}$), 119.9 (Ar-C), 120.2 (Ar-C), 127.0 (Ar-C), 130.0 (Ar-C), 132.3 (Ar-C-Cl), 133.7 (C-C=O), 138.2 (Ar-C-NH), 149.9 (N=C-CH), 159.9 (C=O-NH). ESI-MS: m/z Anal. calcd. for $\text{C}_{12}\text{H}_{12}\text{ClN}_3\text{O}$ ($[\text{M} + \text{H}]^+$): 249.70; found: 250.60.

***N*-(4-Chlorophenyl)-1,3-dimethyl-1*H*-pyrazole-5-carboxamide (4j)**: Colour: pale yellow solid; yield: 62%; m.p.: 181-182 °C, FTIR (KBr, ν_{max} , cm^{-1}): 3352 (NH *str.*), 3010 (Ar-CH *str.*), 2940 (aliph. CH *str.*), 1690 (C=O), 1638 (C=N), 1492 (C=C), 1310 (C-N); ^1H NMR (500 MHz, CDCl_3) δ ppm: 2.34 (s, 3H, CH_3), 3.75 (s, 3H, N- CH_3), 6.40 (s, 1H, $\text{CH}=\text{C}$), 7.42 (ddd, $J = 8.1, 1.6, 0.5$ Hz, 2H, Ar-H), 7.75 (ddd, $J = 8.1, 1.5, 0.5$ Hz, 2H, Ar-H). ^{13}C NMR (300 MHz, CDCl_3) δ ppm: 13.9 (CH_3), 37.7 (N- CH_3), 108.1 ($\text{CH}=\text{C}$), 120.5 (2C, Ar-C), 128.9 (2C, Ar-C), 133.7 (C-C=O), 137.4 (Ar-C-NH), 149.9 (N=C-CH), 159.9 (C=O-NH). ESI-MS: m/z Anal. calcd. for $\text{C}_{12}\text{H}_{12}\text{ClN}_3\text{O}$ ($[\text{M} + \text{H}]^+$): 249.70, found 250.60.

1,3-Dimethyl-*N*-(*p*-tolyl)-1*H*-pyrazole-5-carboxamide (4k): Colour: pale yellow solid; yield: 59%; m.p.: 138-139 °C, FTIR (KBr, ν_{max} , cm^{-1}): 3352 (NH *str.*), 3010 (Ar-CH *str.*), 2940 (aliph. CH *str.*), 1690 (C=O), 1638 (C=N), 1495 (C=C), 1310 (C-N); ^1H NMR (500 MHz, CDCl_3) δ ppm: 2.21 (s, 3H, Ar- CH_3), 2.34 (s, 3H, CH_3), 3.75 (s, 3H, N- CH_3), 6.40 (s, 1H, $\text{CH}=\text{C}$), 7.02-7.16 (7.08 (ddd, $J = 8.1, 1.6, 0.5$ Hz, Ar-H), 7.10 (ddd, $J = 8.1, 1.4, 0.5$ Hz, Ar-H) 4H). ^{13}C NMR (300 MHz, CDCl_3) δ ppm: 13.9 (CH_3), 21.3 (1C, Ar- CH_3), 37.7 (N- CH_3), 108.1 ($\text{CH}=\text{C}$), 117.9 (2C, Ar-C), 129.6 (2C, Ar-C), 133.7 (C-C=O), 137.4 (Ar-C-NH), 141.5 (Ar-C- CH_3), 149.9 (N=C-CH), 159.9 (C=O-NH). ESI-MS: m/z Anal. calcd. for $\text{C}_{13}\text{H}_{15}\text{N}_3\text{O}$ ($[\text{M} + \text{H}]^+$): 229.30; found: 230.25.

***N*-(4-Methoxyphenyl)-1,3-dimethyl-1*H*-pyrazole-5-carboxamide (4l)**: Colour: pale yellow solid; yield: 61%; m.p.: 187-188 °C, FTIR (KBr, ν_{max} , cm^{-1}): 3352 (NH *str.*), 3010 (Ar-

CH *str.*), 2940 (aliph. CH *str.*), 1690 (C=O), 1638 (C=N), 1495 (C=C), 1310 (C-N); ¹H NMR: (500 MHz, CDCl₃) δ ppm: 2.34 (s, 3H, CH₃), 3.75 (s, 3H, N-CH₃), 3.76 (s, 3H, O-CH₃), 6.40 (s, 1H, CH=C), 6.64 (ddd, *J* = 8.8, 2.7, 0.5 Hz, 2H, Ar-H), 7.43 (ddd, *J* = 8.8, 1.7, 0.5 Hz, 2H, Ar-H). ¹³C NMR (300 MHz, CDCl₃) δ ppm: 13.9 (CH₃), 37.7 (N-CH₃), 56.0 (Ar-OCH₃), 108.1 (CH=C), 114.5 (2C, Ar-C), 120.5 (2C, Ar-C), 133.7 (C-C=O), 137.4 (Ar-C-NH), 149.9 (N=C-CH), 159.8 (Ar-C-OCH₃), 159.9 (C=O-NH). ESI-MS: *m/z* Anal. calcd. for C₁₃H₁₅N₃O₂ ([M + H]⁺): 245.30; found: 246.20.

***N*-(3,4-Dimethylphenyl)-1,3-dimethyl-1*H*-pyrazole-5-carboxamide (4m):** Colour: pale yellow solid; yield: 59%; m.p.: 193-194 °C, FTIR (KBr, *v*_{max}, cm⁻¹): 3352 (NH *str.*), 3010 (Ar-CH *str.*), 2940 (aliph. CH *str.*), 1690 (C=O), 1640 (C=N), 1495 (C=C), 1310 (C-N); ¹H NMR (500 MHz, CDCl₃) δ ppm: 2.13-2.24 (6H, 2.18 (s, Ar-CH₃), 2.19 (s, Ar-CH₃), 2.34 (s, 3H, CH₃), 3.75 (s, 3H, N-CH₃), 6.40 (s, 1H, CH=C), 6.60 (dd, *J* = 8.2, 1.8 Hz, 1H, Ar-H), 6.77 (dd, *J* = 8.2, 0.5 Hz, 1H, Ar-H), 7.75 (dd, *J* = 1.8, 0.5 Hz, 1H, Ar-H). ¹³C NMR (300 MHz, CDCl₃) δ ppm: 13.9 (CH₃), 19.9-20.1 (2C, 20.0 (Ar-CH₃), 20.0 (Ar-CH₃), 37.7 (N-CH₃), 108.1 (CH=C), 117.9 (Ar-C), 119.9 (Ar-C), 130.0 (Ar-C-CH₃), 133.4 (Ar-C-CH₃), 133.7 (C-C=O), 138.4 (Ar-C-NH), 149.9 (N=C-CH), 159.9 (C=O-NH). ESI-MS: *m/z* Anal. calcd. for C₁₄H₁₇N₃O ([M + H]⁺): 243.30; found: 244.25.

1,3-Dimethyl-*N*-(4-(trifluoromethyl)phenyl)-1*H*-pyrazole-5-carboxamide (4n): Colour: pale yellow solid; yield: 62%; m.p.: 179-180 °C, FTIR (KBr, *v*_{max}, cm⁻¹): 3352 (NH *str.*), 3010 (Ar-CH *str.*), 2940 (aliph. CH *str.*), 1690 (C=O), 1638 (C=N), 1495 (C=C), 1315 (C-N); ¹H NMR (500 MHz, CDCl₃) δ ppm: 2.34 (s, 3H, CH₃), 3.75 (s, 3H, N-CH₃), 6.40 (s, 1H, CH=C), 7.25 (ddd, *J* = 8.2, 1.4, 0.5 Hz, 2H, Ar-H), 7.57 (ddd, *J* = 8.2, 1.8, 0.5 Hz, 2H, Ar-H). ¹³C NMR (300 MHz, CDCl₃) δ ppm: 13.9 (CH₃), 37.7 (N-CH₃), 108.1 (CH=C), 117.9 (2C, Ar-C), 123.8 (Ar-C-CF₃), 126.5 (2C, Ar-C), 130.3 (CF₃), 133.7 (C-C=O), 137.4 (Ar-C-NH), 149.9 (N=C-CH), 159.9 (C=O-NH). ESI-MS: *m/z* Anal. calcd. for C₁₃H₁₂F₃N₃O ([M + H]⁺): 283.25; found: 284.20.

Anticancer activity

Cell lines and cultures: A 549 (lung), HT 29 (colon), DU 145 (prostate), SiHA (cervical), MCF-7 (breast), B16F10 (mouse skin melanoma) and one normal cell line of human fibroblast were maintained in 90% medium complemented with 10% heat inactivated foetal bovine serum and 100 µg/mL of streptomycin. The cells were incubated at 37 °C in a humidified atmosphere of 5% CO₂ and 95% air in a CO₂ incubator.

Determination of cytotoxicity by MTT assay: After 24 h of attachment on 96-well plates, the cell lines were seeded. Dimethyl sulfoxide (DMSO) was used to create the synthetic chemicals and a 24 h incubation period was required. The cells in the control group were cultured in medium containing 0.2% DMSO. After removing the medium containing the test chemical and washing it with 200 L of PBS, 5 mg/mL of MTT reagent was added to 20 L of washed medium. After that, the reaction was proceeded for 3 h at 37 °C. DMSO (100 µL) were added to the wells to dissolve the purple crystal formazan. The micro-

plate reader was then used to measure the absorbance at 570 nm. The impact of synthesized chemicals on the cell line proliferation was expressed as a percentage of cell viability using the following equation [21]. Each procedure was repeated three times.

$$\text{Cell viability (\%)} = \left(\frac{A_t - A_0}{A_c - A_0} \right) \times 100$$

Molecular docking studies

Protein preparation: Research Collaboratory for Structural Bioinformatics (RCSB) and Protein Data Bank website (<https://www.rcsb.org/>) was used to get the 3D crystal structure of human *c*-Met kinase (PDB: 3F66) and JAK1 (PDB: 3EYG). Protein preparation wizard Schrodinger 2020-3 was used to prepare protein structure. Using the "Protein Preparation Wizard" on Schrodinger 2022-3, we were able to remove the ions (K⁺ and Mg⁺), crystallographic inhibitor and undesired water molecules; assign bond ordering, added polar hydrogens, form disulfide bonds and convert seleno methionine to methionines. In the protein crystal structure, missing atoms were checked and repaired, histidine hydrogens edited, radii was assigned, Kolman charges (-226.847, -27.324) and Gasteiger charges (-21.2368, -226.546) were added and Kollman charge field was set. Ramachandran's plot was used to validate the prepared proteins. Autodock vina was used to create the bioactive conformation. For autodock vina research, PDBQT which is an enhanced format is used for the X, Y and Z coordinates files grid box human *c*-Met kinase (PDB: 3F66) (center x = -0.5403, center y = -23.3503, center z = 28.4090) and JAK1 (PDB: 3EYG) (center x = 10.9888, center y = 14.1857, center z = -14.7729), which contains the partial charges of atoms and atom types. In order to assign the flexible and non-bonded rotation of molecules, torsion angles were calculated. The data collection containing all the chemicals were docked in the protein's active site and Discovery Studio 2021 was used to evaluate the findings.

Ligands selection: ChemDraw was used to create SDF (Structure Data File) 3D versions of all 14 compounds (4a-n). Files in SDF format was converted to PDB using Marvin's drawing. The partial charges of Kollmann and Geister were added with the help of Auto Dock. Selected a torsion tree, increased the number of torsions to 5 and then saved the file in PDBQT 3D format.

Molecular docking: The AutoDock Vina software was used for the genetic algorithm molecular docking study. Auto-dock Vina's virtual screening was accomplished with the help of a Perl script (Command-Perl vina_windows.pl). Docking studies were performed using the human *c*-met kinase (PDB ID: 3FRR) and the Janus kinase 1 (PDB ID: 3EYG) structures. The ligands which were docked then converted to PDB files using PYMOL software so that Biovia Discovery Studio 4.0 could use them in its 2D-3D interactive visualization studies. According to AD Vina scoring, the length of the docked complexes was reduced, if the binding energy (in kcal/mol) was less than the dissociation constant (in pM), with smaller values indicating stronger binding.

RESULTS AND DISCUSSION

Novel pyrazole-5-carboxamides (**4a-n**) were synthesized from ethyl 2,4-dioxopentanoate and methylhydrazine, which are cyclized into ethyl 1,3-dimethyl-1*H*-pyrazole-5-carboxylate (**2**) and 1,3-dimethyl-1*H*-pyrazole-5-carbonyl chloride (**3**), respectively. Finally, intermediate **3** and various substituted arylamines (**a-n**) were condensed in an acidic medium to obtain pyrazole-5-carboxamides (**4a-n**). The yields were in the range of 57-74%. The structure of the synthesized compounds were established from the chemical shift values of the compounds in the NMR analysis. All the chemical shift values of proton NMR and ¹³C NMR are in agreement with the structures. Further *m/z* values of the compounds in the mass spectrum confirmed the formation of the title compounds.

The FT-IR spectrum showed the characteristic band at 3352 cm⁻¹ which indicates the presence of N-H group, presence of aromatic C-H group is indicated by C-H stretching peak at ~3010 cm⁻¹, aliphatic methyl group's C-H is indicated by the band ranging between 2940-2850 cm⁻¹, characteristic band at 1690 cm⁻¹ indicates the presence of C=O group and the pyrazole ring containing C=N, C=C, C-N are indicated by the peaks at ~1698 cm⁻¹, ~1495 cm⁻¹, ~1315 cm⁻¹, respectively.

In ¹H NMR, six aliphatic protons of methyl groups are having chemical shift values ranging from 2.0-3.8 as a singlet. The C-H peak of the pyrazole ring chemical shift value (δ) was observed around δ 6.40-6.42 ppm as a singlet and the four C-H peaks of benzene ring chemical shift value was observed around δ 6.6-7.5 ppm. The chemical shift value (δ) of 13.9 ppm indicates the methyl carbon on the pyrazole ring, while the value of δ 37.7 ppm indicates the methyl carbon present on the nitrogen of pyrazole ring. Most importantly, the chemical shift values (δ) of ~108, ~149, ~133 ppm indicates the three carbons of pyrazole ring.

Anticancer activity: By MTT assay, all the synthesized compounds **4a-n** were tested for their ability to kill cancer

cells in a panel of 7 different cell lines: A 549 (lung), DU 145 (prostate), HT 29 (colon), MCF-7 (breast), SiHA (cervical), B16F10 (mouse skin melanoma) and a normal human fibroblast cell line. The results in Table-1 are denoted as the half maximal inhibitory concentration (IC₅₀ μ M).

For the DU 145 cancer cell line, compounds **4g**, **4j** and **4l** exhibited good anticancer activities with the IC₅₀ values of 14.31 \pm 2.95, 15.20 \pm 2.47 and 15.23 \pm 0.51 μ M, respectively. Whereas compounds **4g**, **4l**, **4k**, **4j** and **4a** inhibited A 549 cell lines with IC₅₀ of 11.66 \pm 2.98, 13.33 \pm 0.45, 13.30 \pm 2.32, 13.79 \pm 2.32 and 16.83 \pm 0.68 μ M. For MCF-7 cell line, compound **4g** showed good anticancer activity with IC₅₀ value 19.14 \pm 0.35 μ M. For HT 29 cell lines, compounds **4g**, **4l** and **4d** displayed good anticancer activity with IC₅₀ 6.646 \pm 1.01, 16.33 \pm 2.39 and 16.17 \pm 0.60 μ M. Against SiHA cancer cell lines, compounds **4g**, **4l**, **4k** and **4j** showed good anticancer activity with IC₅₀ of 5.87 \pm 1.20, 7.92 \pm 0.67, 8.51 \pm 1.45, 10.94 \pm 1.03 μ M, respectively.

Compounds **4j**, **4k** and **4l** exhibited good activity against B16F10 cancer cell lines with IC₅₀ of 14.07 \pm 0.81, 14.26 \pm 1.02 and 15.01 \pm 1.01 μ M. Lastly, for the L929 cancer cell line, compound **4k** with an IC₅₀ value of 24.67 \pm 4.25 μ M presented the good results. For SiHA cancer cell line, compounds **4a**, **4b**, **4j**, **4k**, **4l**, **4m** and **4n** displayed good activity among all the derivatives with IC₅₀ 14.97 \pm 0.60, 15.57 \pm 2.16 10.94 \pm 1.03, 8.51 \pm 1.45, 7.92 \pm 0.67, 12.69 \pm 0.81 and 12.27 \pm 1.99 μ M, respectively. Against MCF-7, L929 derivative **4c** exhibited good activity with IC₅₀ values 44.89 \pm 1.03 and 44.17 \pm 1.83 μ M. Compound **4d** with IC₅₀ 16.33 \pm 2.39 μ M against HT 29, 17.72 \pm 1.12 μ M against SiHA demonstrated a good activity. However, compounds **4e** and **4f** did not showed any anticancer activity against cell lines.

Among all the molecular hybrids, compound **4g** showed excellent anticancer activities with IC₅₀ of 6.646 \pm 1.01 and 5.87 \pm 1.20 μ M, against HT 29 and SiHA cell lines. Compound **4f** showed good activity against A 549 and SiHA cell line with

TABLE-1
ANTIPROLIFERATIVE ACTIVITY (IC₅₀ VALUES) OF COMPOUNDS **4a-n**

Compd. No.	IC ₅₀ (μ M) ^a						
	DU 145	A 549	MCF-7	HT 29	SiHA	B16F10	L929
4a	18.64 \pm 4.73	16.839 \pm 0.68	35.02 \pm 0.52	19.62 \pm 1.49	14.97 \pm 0.60	18.99 \pm 1.94	36.54 \pm 2.53
4b	30.18 \pm 1.33	23.15 \pm 1.05	49.19 \pm 1.20	26.07 \pm 3.32	15.57 \pm 2.16	24.61 \pm 0.52	43.17 \pm 2.95
4c	>100	>100	44.89 \pm 1.03	55.16 \pm 0.67	71.15 \pm 0.52	>100	44.17 \pm 1.83
4d	39.96 \pm 1.83	20.61 \pm 1.01	>100	16.33 \pm 2.39	17.72 \pm 1.12	>100	>100
4e	>100	>100	>100	>100	>100	>100	>100
4f	>100	>100	>100	>100	>100	>100	>100
4g	14.31 \pm 2.95	11.66 \pm 2.98	19.14 \pm 0.35	6.646 \pm 1.01	5.87 \pm 1.20	23.11 \pm 0.51	39.24 \pm 3.74
4h	22.24 \pm 1.10	15.03 \pm 1.27	34.57 \pm 2.10	20.52 \pm 1.05	15.91 \pm 2.06	16.29 \pm 4.69	37.44 \pm 1.26
4i	23.79 \pm 1.86	20.83 \pm 1.02	37.54 \pm 0.69	19.53 \pm 0.77	17.24 \pm 1.01	16.54 \pm 3.74	30.82 \pm 3.74
4j	15.20 \pm 2.47	13.79 \pm 2.32	27.27 \pm 0.97	14.56 \pm 0.51	10.94 \pm 1.03	14.07 \pm 0.81	31.22 \pm 1.12
4k	19.21 \pm 0.90	13.33 \pm 0.45	27.10 \pm 0.51	17.29 \pm 0.99	8.51 \pm 1.45	14.26 \pm 1.02	24.67 \pm 4.25
4l	15.23 \pm 0.51	13.30 \pm 2.32	26.55 \pm 4.25	16.17 \pm 0.60	7.92 \pm 0.67	15.01 \pm 1.01	29.12 \pm 3.74
4m	20.19 \pm 0.99	18.94 \pm 0.45	40.24 \pm 0.69	20.43 \pm 1.72	12.69 \pm 0.81	20.07 \pm 0.67	35.32 \pm 0.69
4n	18.64 \pm 0.51	16.83 \pm 0.52	37.72 \pm 1.01	19.62 \pm 4.25	12.27 \pm 1.99	18.99 \pm 1.12	36.54 \pm 1.03
Doxorubicin ^b	0.98 \pm 1.3	0.87 \pm 2.1	1.02 \pm 0.2	1.1 \pm 0.84	0.91 \pm 0.44	1.3 \pm 0.54	1.12 \pm 0.65

All values are given as means \pm standard deviation.

^aIC₅₀ is the drug concentration effective in inhibiting 50% of the cell growth measured by MTT method.

^bDoxorubicin was used as positive control in this study.

IC₅₀ value of 15.03 ± 1.27 and 15.91 ± 2.06 μM . Compounds **4h** and **4i** also displayed good anticancer activity against SiHA with IC₅₀ of 15.91 ± 2.06 , 17.24 ± 1.01 and B16F10 with IC₅₀ of 16.29 ± 4.69 , 16.54 ± 3.74 μM . All the compounds IC₅₀ values were compared with standard anticancer drug doxorubicin, unfortunately, none of the synthesized compounds is as good as the standard drug.

From the anticancer results, it is concluded that substituents groups on phenyl ring affected the activity of the compounds **4g** (3-F), **4j** (4-Cl), **4l** (-OCH₃), which have electron-donating and moderate electron withdrawing groups and thus exhibiting the good activity. Similarly, compounds which have electron withdrawing groups **4e** and **4f** (3-NO₂, 4-NO₂) displayed poor activity.

Molecular docking studies: Among all the titled compounds, compounds **4c** and **4j** showed a good binding score (-7.2 and -7.1 Kcal/mol) against 3F66, which is similar to the Ruxolitinib binding score (-7.4 kcal/mol). Compounds **4c**, **4a** and **4m** displayed good binding affinity (-7.2 and -6.9 Kcal/mol) against 3EYG Protein compared to standard Ruxolitinib (-6.9 kcal/mol). Table-2 depicts the docking scores of the synthesized compounds.

Molecular docking studies against human c-Met kinase (PDB: 3F66): Among the synthesized 14 compounds, compound **4c** showed the highest binding affinity -7.2 kcal/mol, as compared to reference drug Ruxolitinib binding affinity -7.4 kcal/mol for human c-Met kinase (PDB: 3F66), the reason could be the formation of hydrogen bond with water molecule at active site as reference compound. Compound **4c** forms two conventional hydrogen bonds with one water molecule and amino acids Asp 1231. One pi-donor hydrogen bond with 1230. Hydrophobic interactions with ala1221, leu 1157, lys1110, val 1092 and met 1211, whereas compound **4d** showed a binding affinity -6.9 kcal/mol and made a total of three H bonds. Among

TABLE-2 DOCKING SCORE OF THE SYNTHESIZED COMPOUNDS		
Compound	Binding affinity (-kcal/mol)	
	3F66	3EYG
4a	5.7	6.9
4b	6.4	6.8
4c	7.2	7.3
4d	6.9	6.8
4e	6.3	5.4
4f	5.7	5.9
4g	6.9	6.5
4h	6.5	6.5
4i	5.4	5.8
4j	7.1	6.4
4k	5.8	5.7
4l	5.3	6.3
4m	6.2	6.9
4n	5.3	5.1
Ruxolitinib	7.4	6.9

these, two are conventional H-bonds with arg 1086 and tyr 1230. Hydrophobic interactions of **4d** with ala1221, ala1226, val1092 and tyr1230 were observed. Compound **4n** showed the lowest binding affinity of -5.3 kcal/mol. The reason could be that it does not make any H bonds with protein. Compound **4n** forms halogen bonds with amino acids leu1225, arg 1227 and arg 1227. Fig. 1 represents the 3D binding interactions of some selected compounds against human c-Met kinase.

Molecular docking studies against JAK1 (3EYG): Among the synthesized 14 compounds, compound **4c** showed the highest binding affinity of -7.3 kcal/mol, as compared to reference drug Ruxolitinib binding affinity of -6.9 kcal/mol for JAK1 (3EYG). The reason could be the formation of hydrogen bonds with water molecules at active sites as reference compound. Compound **4c** forms a conventional hydrogen bond with

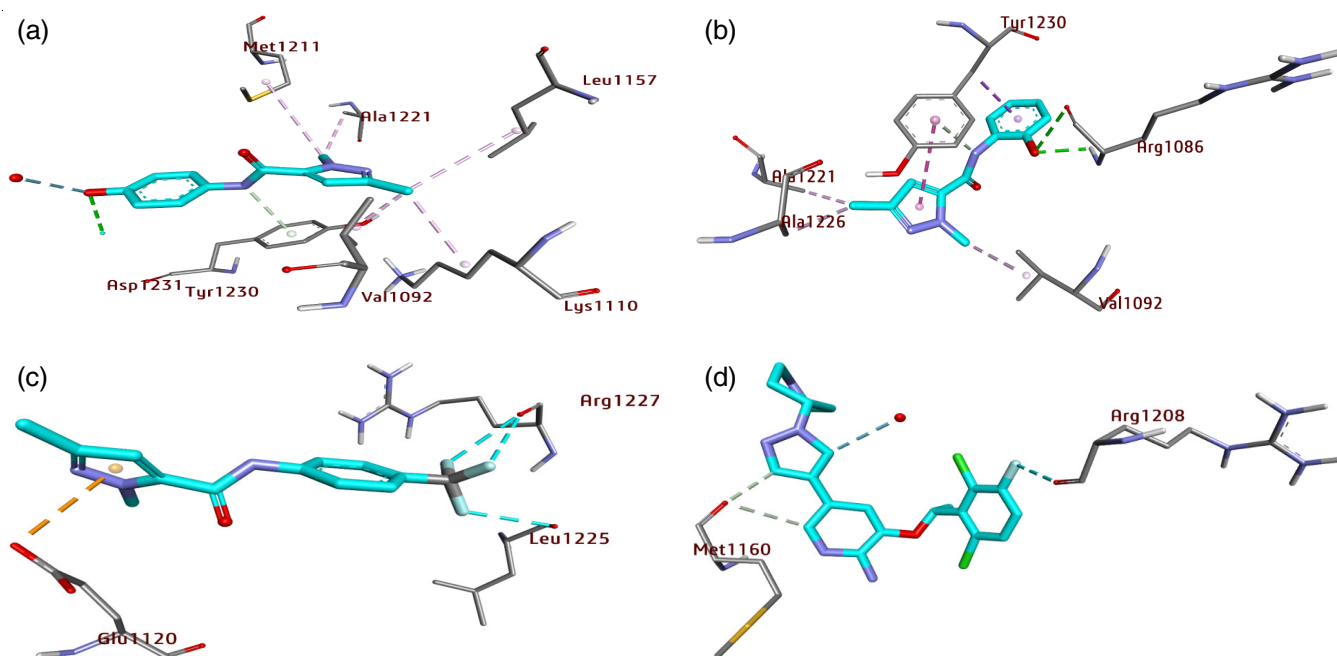


Fig. 1. 3D interaction of some selected compounds **4c** (a), **4d** (b), **4n** (c), ruxolitinib (d), against human c-Met kinase

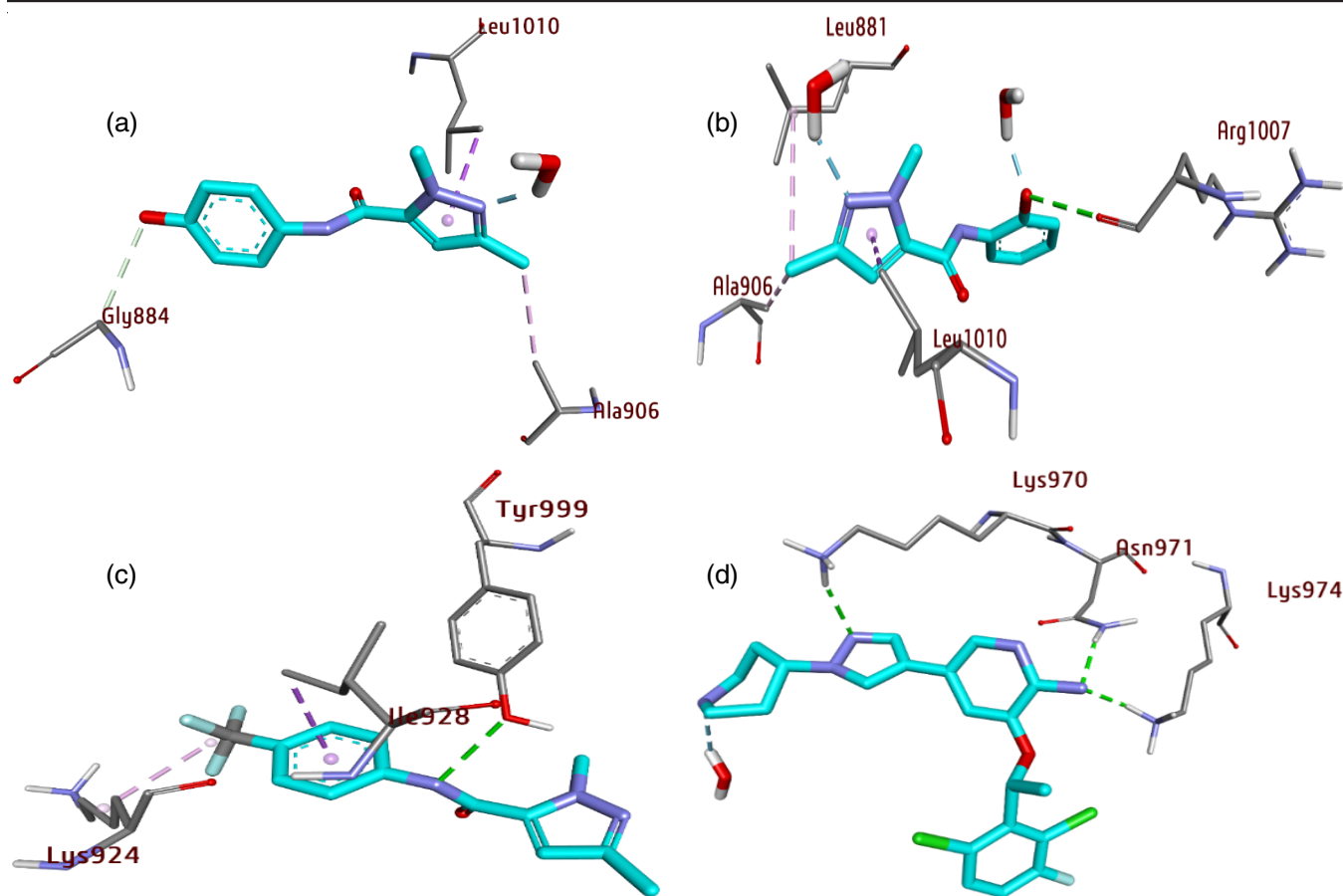


Fig. 2. 3D interaction of some selected compounds **4c** (a), **4d** (b), **4n** (c), ruxolitinib (d), against JAK1

water molecule and carbon hydrogen bond with gly 884 amino acid, while the hydrophobic interaction with ala906 and leu 1010. Compound **4d** showed binding affinity of -6.8 kcal/mol, as compared to reference drug for JAK1 (**3EYG**). Compound **4d** forms three conventional hydrogen bonds with two water molecules and amino acid arg 1007, pi-sigma bonds with leu 1010, one alkyl-alkyl with ala906 and one with a pi-alkyl leu881. Compound **4n** showed the lowest binding affinity of -5.1 kcal/mol as compared to reference drug Ruxolitinib binding affinity of -6.9 kcal/mol for JAK1 (**3EYG**), whereas compound **4n** forms the conventional hydrogen bonds with amino acids tyr 999 and hydrophobic interaction with lys 924 and ile 928. It forms total of four conventional hydrogen bonds with one water molecule and amino acids lys 970, asn971 and lys974. Fig. 2 represents the 3D binding interactions of some selected compounds against JAK1.

Conclusion

In conclusion, the synthesis and characterization of a new series of pyrazole carboxamide hybrids (**4a-n**) from readily accessible commercial starting materials and an economically viable approach is reported. The MTT assay was used to test the efficacy of the synthesized compounds for *in vitro* anticancer activity. Compounds **4g**, **4j** and **4l** showed moderate potent anticancer activity as measured by their IC_{50} values in comparison to those of conventional drugs. All the compounds showed good binding scores in molecular docking studies.

The synthesized compounds may offer valuable therapeutic intervention for the cancer treatment.

CONFLICT OF INTEREST

The authors declare that there is no conflict of interests regarding the publication of this article.

REFERENCES

- Global Cancer Report-2018, International Agency for Research on Cancer, WHO report September (2021).
- J.K. De Martino and D.L. Boger, *Drugs Future*, **33**, 969 (2008); <https://doi.org/10.1358/dof.2008.033.11.1247542>
- W.J. Curran, *Oncology*, **63**, 29 (2002); <https://doi.org/10.1159/000067145>
- K. Nurgali, R.T. Jagoe and R. Abalo, *Front. Pharmacol.*, **9**, 245 (2018); <https://doi.org/10.3389/fphar.2018.00245>
- Y. Hu and J. Bajorath, *J. Chem. Inf. Model.*, **51**, 3138 (2011); <https://doi.org/10.1021/ci200461w>
- M. Skoreński and M. Sieńczyk, *Pharmaceuticals*, **14**, 1164 (2021); <https://doi.org/10.3390/ph14111164>
- G. Ion, O. Olaru, G. Nitulescu, I. Olaru, A. Tsatsakis, T. Burykina, D. Spandidos and G. Nitulescu, *Oncol. Rep.*, **44**, 589 (2020); <https://doi.org/10.3892/or.2020.7636>
- R.F. Costa1, L.C. Turones, K.V.N. Cavalcante, I.A. Rosa Jr., C.H. Xavier, L.P. Rosseto, H.B. Napolitano, P.F. da Silva Castro, M.L. Ferreira-Neto, G.M. Galvão, R. Menegatti, G.R. Pedrino, E.A. Costa, J.L. Rodrigues-Martins and J.O. Fajemiroye, *Front. Pharmacol.*, **12**, 666725 (2021); <https://doi.org/10.3389/fphar.2021.666725>
- M. Chalkha, M. Bakhouch, M. Akhazzane, M. Bourass, Y. Nicolas, G. Al Houari and M. El Yazidi, *J. Chem. Sci.*, **132**, 86 (2020); <https://doi.org/10.1007/s12039-020-01792-3>

10. A. Petrou, M. Fesatidou and A. Geronikaki, *Molecules*, **26**, 3166 (2021); <https://doi.org/10.3390/molecules26113166>
11. H. Kumar, D. Saini, S. Jain and N. Jain, *Eur. J. Med. Chem.*, **70**, 248 (2013); <https://doi.org/10.1016/j.ejmech.2013.10.004>
12. M. Albratty and H. Alhazmi, *Arab. J. Chem.*, **15**, 103846 (2022); <https://doi.org/10.1016/j.arabjc.2022.103846>
13. E. Mohamed, N. Ismail, M. Hagras and H. Refaat, *Future J. Pharm. Sci.*, **7**, 1 (2021); <https://doi.org/10.1186/s43094-020-00165-4>
14. G. Nitulescu, *Molecules*, **27**, 3300 (2022); <https://doi.org/10.3390/molecules27103300>
15. B. Poudyal and Bharghav, *National J. Pharm. Sci.*, **1**, 34 (2021).
16. P. Bose and S. Verstovsek, *Hemasphere*, **4**, e424 (2020); <https://doi.org/10.1097/HS9.0000000000000424>
17. P. Cohen, D. Cross and P.A. Jänne, *Nat. Rev. Drug Discov.*, **20**, 551 (2021); <https://doi.org/10.1038/s41573-021-00195-4>
18. D. Kralj, M. Friedrich, U. Grošelj, S. Kiraly-Potpara, A. Meden, J. Wagger, G. Dahmann, B. Stanovnik and J. Svete, *Tetrahedron*, **65**, 7151 (2009); <https://doi.org/10.1016/j.tet.2009.06.021>
19. M. Samet, R. Kasimogullari and S. Ok, *J. Postdr. Res.*, **2**, 64 (2014).
20. R. Ohno, A. Watanabe, T. Matsukawa, T. Ueda, H. Sakurai, M. Hori and K. Hirai, *J. Pestic. Sci.*, **29**, 15 (2004); <https://doi.org/10.1584/jpestics.29.15>
21. Z. Pourramezan, M. Oloomi and R. Kasra-Kermanshahi, *Int. J. Prev. Med.*, **11**, 132 (2020); https://doi.org/10.4103/ijpvm.IJPVM_307_19